Journal of Biomechanics 45 (2012) 1406–1413

Contents lists available at SciVerse ScienceDirect

Journal of Biomechanics

journal homepage: www.elsevier.com/locate/jbiomech
www.JBiomech.com

Sensitivity of maximum sprinting speed to characteristic parameters of the muscle force–velocity relationship

Ross H. Miller*, Brian R. Umberger, Graham E. Caldwell

Department of Kinesiology, University of Massachusetts Amherst, MA, USA

ARTICLE INFO

Article history:
Accepted 21 February 2012

Keywords:
Sprinting
Speed limit
Muscle
Force–velocity relationship
Simulation
Forward dynamics
Hill model

ABSTRACT

An accumulation of evidence suggests that the force–velocity relationship (FVR) of skeletal muscle plays a major role in limiting maximum human sprinting speed. However, most of the theories on this limiting role have been non-specific as to how the FVR limits speed. The FVR is characterized by three parameters that each have a different effect on its shape, and could thus limit sprinting speed in different ways: the maximum shortening velocity V_{max}, the shape parameter A_R, and the eccentric plateau C_{ecc}. In this study, we sought to determine how specifically the FVR limits sprinting speed using forward dynamics simulations of human locomotion to examine the sensitivity of maximum speed to these three FVR parameters. Simulations were generated by optimizing the model's muscle excitations to maximize the average horizontal speed. The simulation's speed, temporal stride parameters, joint angles, GRF, and muscle activity in general compared well to data from human subjects sprinting at maximum effort. Simulations were then repeated with incremental and isolated adjustments in V_{max}, A_R, and C_{ecc} across a physiological range. The range of speeds (5.22–6.91 m s^{-1}) was most sensitive when V_{max} was varied, but the fastest speed of 7.17 m s^{-1} was attained when A_R was set to its maximum value, which corresponded to all muscles having entirely fast-twitch fibers. This result was explained by the muscle shortening velocities, which tended to be moderate and within the range where A_R had its greatest effect on the shape of the FVR. Speed was less sensitive to adjustments in C_{ecc}, with a range of 6.23–6.70 m s^{-1}. Increases in speed with parameter changes were due to increases in stride length more so than stride frequency. The results suggest that the shape parameter A_R, which primarily determines the amount of muscle force that can be produced at moderate shortening velocities, plays a major role in limiting the maximum sprinting speed. Analysis of muscle force sensitivity indicated support for previous theories on the time to generate support forces in stance (Weyand et al., 2000, Journal of Applied Physiology, 89, 1991–1999) and energy management of the leg in swing (Chapman & Caldwell, 1983, Journal of Biomechanics 16, 79–83) as important factors in limiting maximum speed. However, the ability of the knee flexors to slow the rotational velocity of the leg in preparation for footstrike did not appear to play a major role in limiting speed.

© 2012 Elsevier Ltd. All rights reserved.

1. Introduction

A central question in the study of sprint running is how modifiable factors such as muscular properties limit the maximum steady-state speed. In a previous study (Miller et al., 2011a), we identified the force–velocity relationship of muscular force production (Hill, 1938) as the most critical muscle contractile property in maximum sprinting speed, supporting a similar conclusion drawn 85 years ago by Furusawa et al. (1927) and later assessed by Fenn (1930a,b). In the present study, we ask how specific features of the force–velocity relationship limit maximum sprinting speed.

The force–velocity relationship described by Hill (1938) and by Katz (1939) includes constants A and B that define the shape of the concentric limb. The ratio B/A specifies the maximum shortening velocity V_{max}. On the eccentric limb, the plateau force F_{ecc} is typically scaled by the maximum isometric force F_o to give the dimensionless parameter C_{ecc}. Independent changes in these parameters have different effects on the shape of the force–velocity relationship. A primarily affects the shape at moderate velocities, V_{max} (or B) the shape at fast concentric velocities, and C_{ecc} the height of the eccentric limb (Fig. 1). These characteristic parameters can potentially constrain the maximum sprinting speed by limiting the amount of force muscles can produce during particular points in the stride. Two theories on how the

* Correspondence to: 6-208 Apps Medical Research Centre, Queen's University, Kingston, ON, Canada K7L2V7. Tel.: +1 613 549 6666; fax: +1 613 549 2529.
E-mail addresses: rosshm@gmail.com, ross.miller@queensu.ca (R.H. Miller).

0021-9290/$ - see front matter © 2012 Elsevier Ltd. All rights reserved.
doi:10.1016/j.jbiomech.2012.02.024

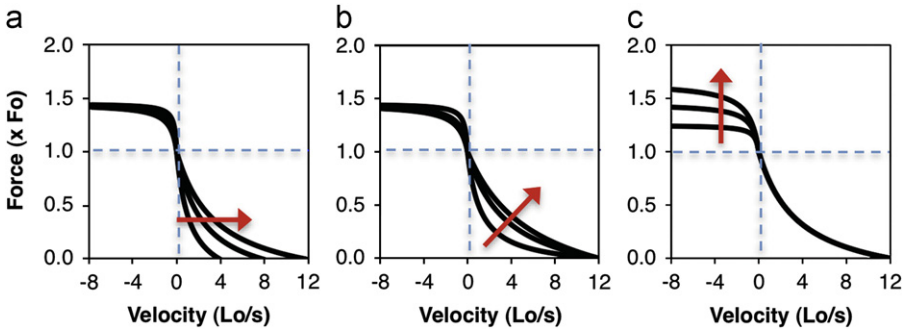

Fig. 1. Sensitivity of the muscle force–velocity relationship to incremental adjustments in (a) the maximum shortening velocity, (b) the dynamic constant A, and (c) the eccentric plateau force. Arrows indicate trend directions for increasing parameter magnitude. Axes are scaled by the optimal contractile component length (L_o) and the maximum isometric force (F_o). The crosshair indicates zero velocity and maximum isometric force. Graphs were constructed using the equations of van Soest and Bobbert (1993).

force–velocity relationship limits maximum sprinting speed have been proposed. The stance-based "time to generate force" theory of Weyand et al. (2000, 2010) states that speed is limited by the rate at which muscles can develop sufficient forces to support the body weight while the large extensor muscles are rapidly shortening, implicating the concentric force–velocity relationship. The swing-based "energy management" theory of Chapman and Caldwell (1983) poses that speed is limited by the ability of the knee flexors to reduce the kinetic energy of the lower limb while they lengthen in late swing, implicating the eccentric force–velocity relationship. These two theories are not necessarily in conflict, but it is unknown if one or the other plays a predominant role in limiting maximum sprinting speed. Analyses of muscle forces produced in stance and swing while the characteristic force–velocity parameters are manipulated should help clarify this issue.

Therefore, our purpose was to examine the sensitivity of maximum sprinting speed to adjustments in the characteristic force–velocity parameters. The force–velocity relationship in human muscle is sensitive to training status (e.g. Thorstensson et al., 1977; Andersen et al., 2005), but it is impossible to modify selected parameters *in vivo*, or to account for other confounding training effects such as increased muscle strength. We therefore used computer simulations to determine the effects of incremental adjustments in force–velocity parameter values on maximum sprinting speed. We expected that increasing the parameter values of A, V_{max}, or C_{ecc} would increase maximum sprinting speed, and hypothesized that maximum speed would be most sensitive to adjustments in V_{max} because sprinting presumably requires muscles to shorten at fast velocities. Finally, we assessed the simulation results in the context of the Weyand et al. (2000, 2011) and Chapman and Caldwell (1983) theories to elucidate their respective roles in limiting maximum sprinting speed.

2. Methods

2.1. Experimental data

Kinematic, ground reaction force (GRF), and muscle electromyographic (EMG) data were collected from 12 adult females (mean ± SD: age = 27 ± 6 years, height = 1.66 ± 0.05 m, mass = 61.0 ± 4.7 kg) as they sprinted at maximum effort along a level 40-m runway (Miller et al., 2011a). Subjects were fit and recreationally active but were not competitive sprint athletes. Data were measured from one stride near the center of the runway, ~20 m from the starting point.

Reflective marker positions were smoothed at 12 Hz and processed into 2D histories of sagittal plane joint and segment kinematics (Robertson et al., 2004). Raw EMG signals were processed into linear envelopes by sequentially applying a bandpass filter (20–300 Hz), full-wave rectification, and a lowpass filter (10 Hz), with amplitudes scaled to maximum isometric contractions. All data were averaged over strides (five per subject), then over subjects.

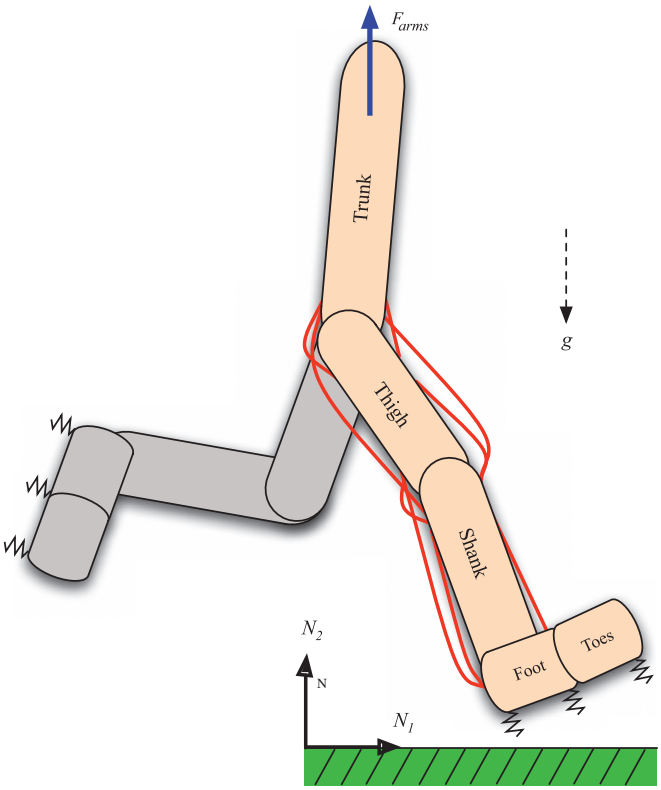

Fig. 2. Diagram of the 2D computer model used to simulate sprinting.

2.2. Computer model

A previously described 2D model was used to simulate sprinting (Fig. 2; Miller et al., 2011a,b). The model included nine rigid segments (trunk and bilateral thighs, shanks, feet, and toes) actuated by 18 Hill-based muscle models (bilateral iliopsoas, glutei, vasti, biceps femoris (short head), tibialis anterior, soleus, rectus femoris, hamstrings, and gastrocnemius), each with a contractile component (CC) in series with an elastic component (SEC). The muscle model parameters (Table 1) were derived from isovelocity joint strength tests on the female runners. The muscle force–velocity equations of van Soest and Bobbert (1993) were used, with the dimensionless Hill constants A_R and B_R defined according to Winters and Stark (1985, 1988)

$$A_R = \frac{A}{F_o} = 0.1 + 0.4FT \quad (1)$$

$$B_R = \frac{B}{L_o} = A_R V_{max} \quad (2)$$

where FT is the proportion of fast-twitch muscle fibers, F_o is the maximum isometric muscle force, and L_o is the optimal CC length. Eq. (2) is used to calculate B_R given values for A_R and V_{max}. Non-linear spring/frictional elements on the feet

simulated ground contact (Miller et al., 2011a). Passive torsional spring-dampers restricted the joints to realistic ranges of motion (Riener and Edrich, 1999). The effect of arm swing was modeled as a vertical sinusoidal force applied to the trunk (Miller et al., 2009). A model of human muscle energy expenditure (Umberger et al., 2003; Umberger, 2010) was used to calculate the metabolic cost of transport in the simulations.

Time-varying excitation signals to each muscle were piecewise linear functions of 21 nodal values spaced evenly over one stride cycle, with the first and last nodes equal in magnitude. Bilateral muscle excitation patterns were identical but temporally shifted by half the stride duration.

2.3. Simulations

One stride of sprinting was simulated using a parallel simulated annealing algorithm (Higginson et al., 2005) that optimized the model's control variables to maximize the quantity J

$$J = \frac{\Delta x_{CoM}}{t_f} - (0.01\varepsilon_\theta + 0.0001\varepsilon_\omega + 0.001\varepsilon_{pas} + \varepsilon_{grf}) \quad (3)$$

where Δx_{CoM} is the horizontal displacement of the center of mass over the stride duration t_f. The bracketed terms are penalty functions, with ε_θ and ε_ω being the squared differences between the initial and final segment angular positions and velocities, respectively, to encourage periodicity. ε_{pas} is the sum of the squared passive joint moment integrals, to discourage extreme joint angles. ε_{grf} is the ratio of braking (B_{imp}) and propelling (P_{imp}) impulses from the horizontal GRF, to encourage a steady speed

$$\varepsilon_{grf} = \left[\frac{\max(B_{imp}, P_{imp})}{\min(B_{imp}, P_{imp})}\right]^2 - 1 \quad (4)$$

The penalty weighting coefficients were the smallest values that produced nearly periodic strides. To reduce computational time, one step from right to left foot contact was simulated, assuming bilateral symmetry to reconstruct the complete stride (Anderson and Pandy, 2001). The control variables were the 180 nodal muscle excitation magnitudes, the amplitude and phase shift of the arm swing force, the angular stiffness of the metatarsal joints, and the stride duration. Initial muscle model state variables were defined according to Neptune et al. (2001). The initial generalized coordinates and speeds were allowed to vary as controls within a range of ± 2 standard deviations of the experimental mean. Any optimization that converged with an initial horizontal hip velocity above 98% of the permitted upper bound was repeated with a higher upper bound.

An initial simulation with the nominal force–velocity parameters from Miller et al. (2011a) (Table 1; $V_{max}=12\,L_o\,s^{-1}$ and $C_{ecc}=1.45$ for all muscles) was compared to the experimental data to establish the model's capability for realistic sprinting. Next, simulations were performed with each of the three force–velocity parameters adjusted for all muscles across their full physiological ranges (e.g. Zajac, 1989; Andersen et al., 2005). A_R was adjusted from 0.1 (100% slow-twitch fibers) to 0.5 (100% fast-twitch) in increments of 0.1 (Eq. 1). V_{max} was adjusted from 4 to 14 $L_o\,s^{-1}$ in increments of 2 $L_o\,s^{-1}$ (e.g. Domire & Challis, 2010). C_{ecc} was adjusted from 1.25 to 1.65 in increments of 0.10 (e.g. Zajac, 1989). When one parameter was adjusted, the others were held at their nominal values.

Table 1
Nominal muscle model parameters important for the force–velocity relationship. F_o=maximum isometric force; L_o=optimal contractile component length; FT=percentage of fast-twitch muscle fibers; A_R and B_R=relative force–velocity constants.

Muscle	F_o (N)	$PCSA$ (cm^2)	L_o (cm)	FT (%)	A_R	B_R (s^{-1})
Iliopsoas	2324	58.1	12.0	52	0.31	3.70
Glutei	4072	101.8	14.0	47	0.29	3.46
Vasti	5664	141.6	9.5	59	0.34	4.03
Biceps femoris (short head)	1008	25.2	14.5	31	0.22	2.69
Tibialis anterior	2680	67.0	8.8	25	0.20	2.40
Soleus	5888	147.2	4.9	19	0.18	2.11
Rectus femoris	1464	36.6	11.0	67	0.37	4.42
Hamstrings	3000	75.0	14.0	41	0.26	3.17
Gastrocnemius	2816	70.4	7.1	50	0.30	3.60

3. Results

3.1. Subject performance

The mean speed, stride length and stride frequency of the subjects were 6.42 ± 0.61 m s^{-1}, 3.21 ± 0.30 m, and 2.01 ± 0.24 Hz, respectively. The joint angles and GRF (Fig. 3) and EMG timing (Fig. 4) were consistent with other sprinting studies (Mann and Hagy, 1980; Thelen et al., 2005).

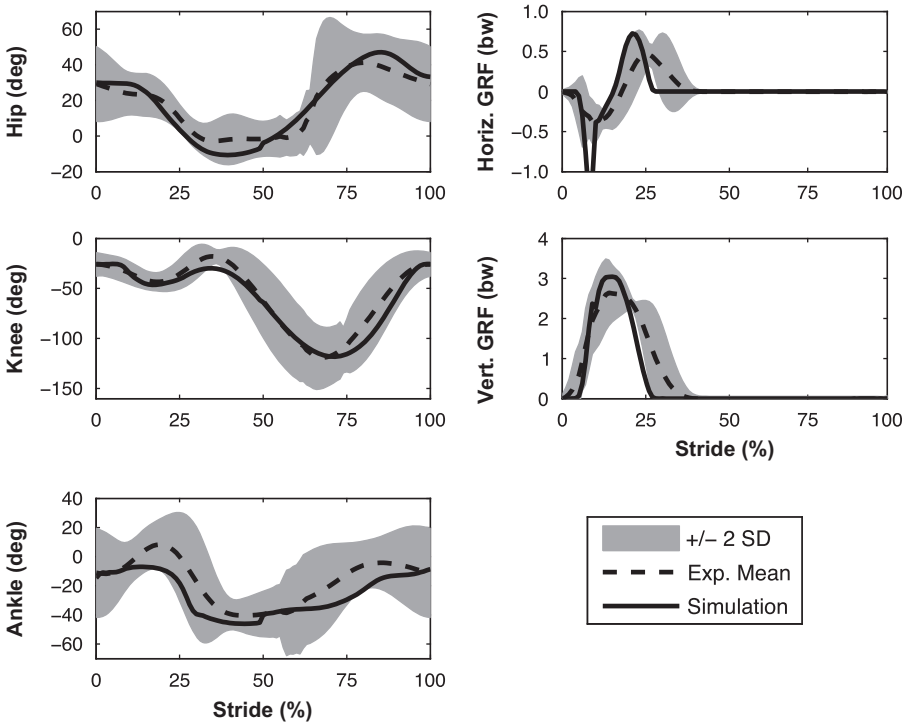

Fig. 3. Joint angles and GRF components vs. the stride cycle from the humans subjects (dashed lines) and the initial sprinting simulation (solid lines). Shaded area is +/− two between-subjects standard deviations around the mean of the human subjects. The stride begins and ends at initial contact of the right foot.

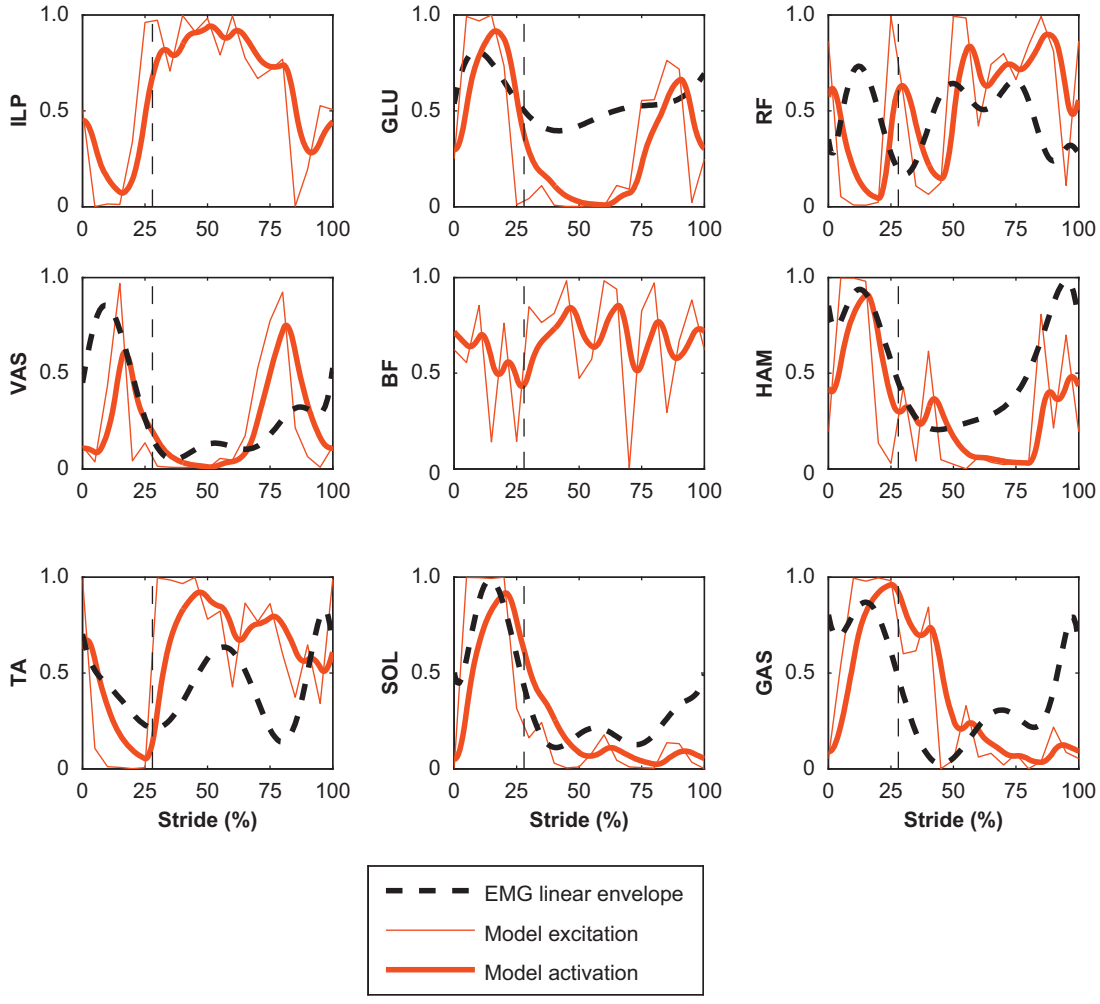

Fig. 4. Optimized muscle excitations (thin lines) and activations (thick lines) from the initial sprinting simulation compared to the EMG linear envelopes (dashed lines). ILP=iliopsoas; GLU=glutei; BF=biceps femoris (short head); TA=tibialis anterior; SOL=soleus; RF=rectus femoris; HAM=hamstrings; GAS=gastrocnemius. The stride begins and ends at initial contact of the right foot. Vertical dashed lines indicate toe-off.

3.2. Nominal simulation

The nominal simulation sprinted at 6.75 m s^{-1}, 5% faster than the subject mean. The stride length and stride frequency were 3.39 m and 1.99 Hz. The joint angles and GRF (Fig. 3) generally fell within two between-subjects standard deviations of the experimental means (average deviation=1.71 SD), despite not being tracked explicitly in the simulation. The simulated stance duration (28% of the stride) was shorter than the subject mean (37 ± 5%) but within the range observed (26–42%). The peak braking force exceeded the human range, but the braking and propelling impulses were still of equal magnitude. Zero lag cross-correlations between the muscle model activations and linear envelopes (Fig. 4) averaged 0.60, similar to the cross-correlations between linear envelopes for the individual human subjects (average 0.65). The metabolic cost of transport was 5.52 J m^{-1} kg^{-1}, which is reasonably close to *in vivo* human estimates by Weyand and Bundle (2005; their Fig. 3), whose data suggest a cost of transport of ~5.5 J m^{-1} kg^{-1} for running at ~7 m s^{-1}, assuming 5 kcal per liter of oxygen equivalent consumed.

3.3. Sensitivity to force–velocity parameters

The sensitivity of the simulation's speed, stride length, and stride frequency varied depending on the parameter manipulated (Fig. 5), with speed ranging from 5.22 to 7.17 m s^{-1} overall. The average deviations from periodicity were 2.5° for the joint angles, 15.9° s^{-1} for the joint angular velocities, and 0.1 m s^{-1} for the hip velocities. As V_{max} increased from 4 to 14 L_o s^{-1}, the sprinting speed increased from 5.22 to 6.91 m s^{-1}. A_R adjustments from 0.1 to 0.5 increased speed from 5.60 to 7.17 m s^{-1}. C_{ecc} adjustments from 1.25 to 1.65 caused smaller speed increases from 6.23 to 6.70 m s^{-1}. Overall, greater stride length accounted for 78% of the speed increases associated with incremental parameter increases. Across all simulations, the stance phase duration ranged from 25 to 28% of the stride duration and showed an inconsistent relationship with speed (p=0.45, R^2=0.19). The metabolic cost ranged from 5.40 to 5.66 J m^{-1} kg^{-1}, and was not correlated with speed (p=0.55, R^2=0.11).

Time histories of CC velocities and muscle forces at each parameter value are presented in the Electronic Supplementary Material (Figs. S1-S6). In general, CC velocities were insensitive to parameter modifications, particularly to changes in A_R and C_{ecc}. Soleus was the only muscle that operated within 1L_o s^{-1} of its maximum shortening velocity, briefly after toe-off. The peak shortening velocities of soleus and gastrocnemius increased with increasing V_{max} (Fig. S1), but otherwise peak CC velocities displayed no systematic relationships with force–velocity parameter values.

For similar CC velocities, the force–velocity relationship predicts larger potential muscle forces as parameter values increase (Fig. 1). The average forces generated by some muscles during

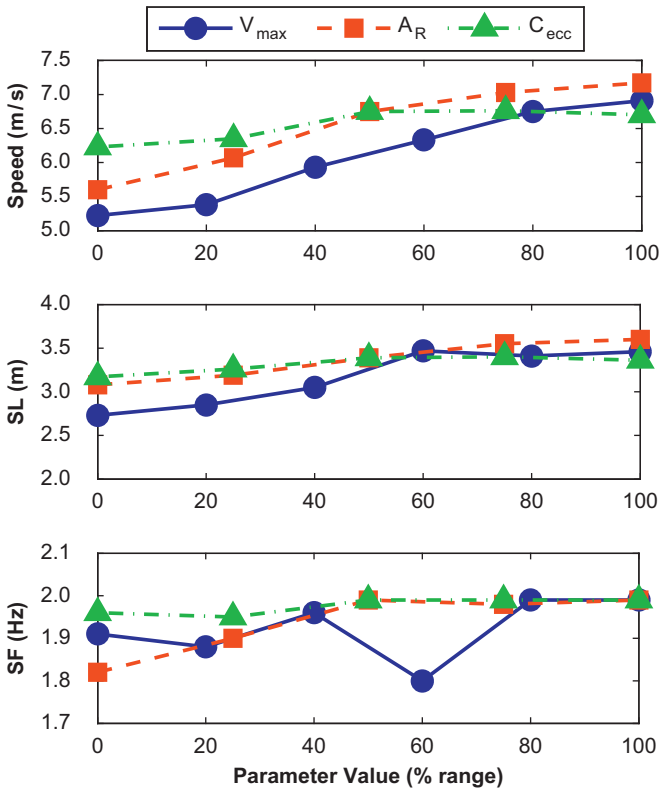

Fig. 5. Sensitivity of sprinting speed, stride length (SL), and stride frequency (SF) to adjustments in the maximum shortening velocity V_{max} (circles), the dynamic constant A_R (squares), and the eccentric plateau C_{ecc} (triangles).

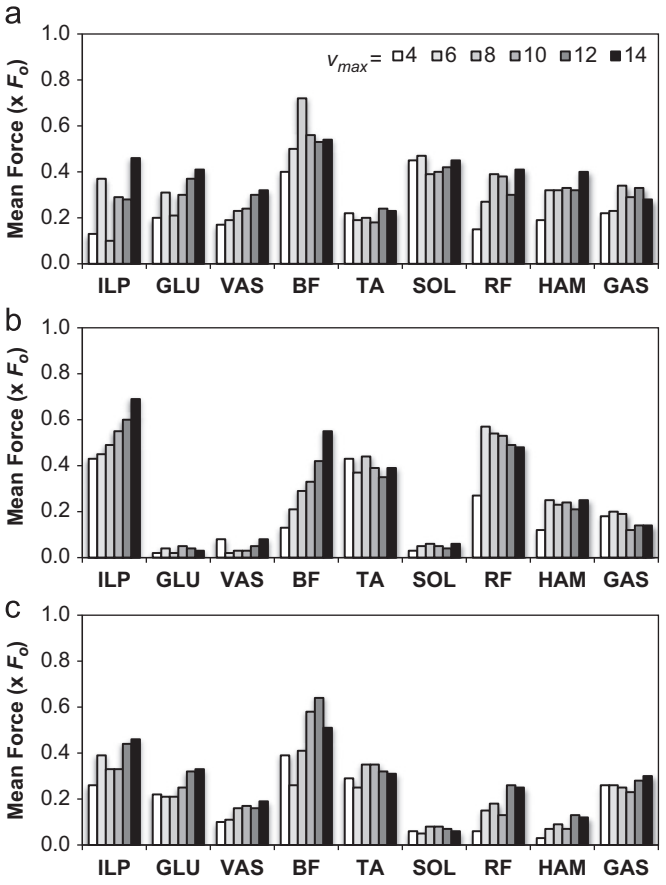

Fig. 6. Average (mean) muscle forces during (a) stance, (b) the first 50% of swing, and (c) the last 50% of swing as V_{max} was increased incrementally from 4 to 14 $L_o\ s^{-1}$. Darker shaded bars indicate greater V_{max} values. Force are scaled by F_o. Muscle abbreviations are as in Fig. 4.

stance, early swing, and late swing supported this prediction. For example, each increase in V_{max} increased the average vasti force during stance but not swing (Fig. 6). The average iliopsoas and biceps femoris forces increased with each increase in V_{max} during early swing, but not during late swing or stance. For the other muscles, average forces tended to increase as V_{max} increased, but the relationship was not monotonic for any stride phase.

During stance, successive increases in A_R increased the average force in six of the nine muscles (Fig. 7). Iliopsoas and rectus femoris forces increased monotonically with increasing A_R during both early and late swing, as did biceps femoris during early swing only. Other muscle forces had more complex relationships with A_R, such as glutei and biceps femoris in late swing, with increased forces from A_R=0.1 to 0.3 but lower forces with further increases.

Average muscle forces were less sensitive to changes in C_{ecc} (Fig. 8), with no consistent patterns for any muscle during stance. However, during early swing the average biceps femoris force increased with each increase in C_{ecc}, as did the average iliopsoas force in late swing. During late swing, the glutei force increased as C_{ecc} rose until reaching a plateau at C_{ecc}=1.45.

4. Discussion

There is ample evidence that the force–velocity relationship limits human sprinting performance, including theory (Furusawa et al., 1927), experiments (Weyand et al., 2000), computer simulations (Lee & Piazza, 2009), and conclusions from systematic reviews (van Ingen Schenau et al., 1994). In the present study, we expanded on these general conclusions by examining how particular force–velocity parameters affect speed and muscle force production in human sprinting simulations. The muscle model parameters were derived from data on live humans, and comparisons between the nominal simulations and human runners were reasonable even though the experimental data were not tracked explicitly (Figs. 3 and 4). Thus, we suspect the modeled muscle forces and kinematics are likely similar to those generated by sprinting humans. However, the results should be interpreted cautiously, given the limitations associated with a simplified 2D musculoskeletal model.

All three parameters (V_{max}, A_R, and C_{ecc}) increased the maximum sprinting speed when adjusted over a physiological range. The maximum shortening velocity V_{max} primarily affects the force produced at the fastest shortening velocities, the A_R mainly affects the force produced at moderate velocities, and the eccentric parameter C_{ecc} affects the force generated during CC lengthening. For all parameters, the resulting speed increase was due primarily to a longer stride length rather than a greater stride frequency. Aside from cases where V_{max} was very low, the CC velocities were relatively unaffected by parameter value adjustments; speed increased because the greater parameter values (Fig. 1) allowed muscles to generate greater forces at similar CC velocities (Figs. 6–8). The maintenance of CC velocities despite faster running speeds is facilitated by SEC compliance and CC-SEC dynamics, which permit the CC and whole-muscle kinematic states to differ (Alexander, 2002; Hof, 2003); faster leg motions do not necessarily require faster CC velocities.

Sprinting speed increased linearly as A_R (R^2=0.93) and V_{max} (R^2=0.98) increased, with the fastest speed (7.17 m s^{-1}) achieved with A_R at its maximum value of 0.5. These results are consistent with the simulated muscle kinematics: although both A_R and V_{max}

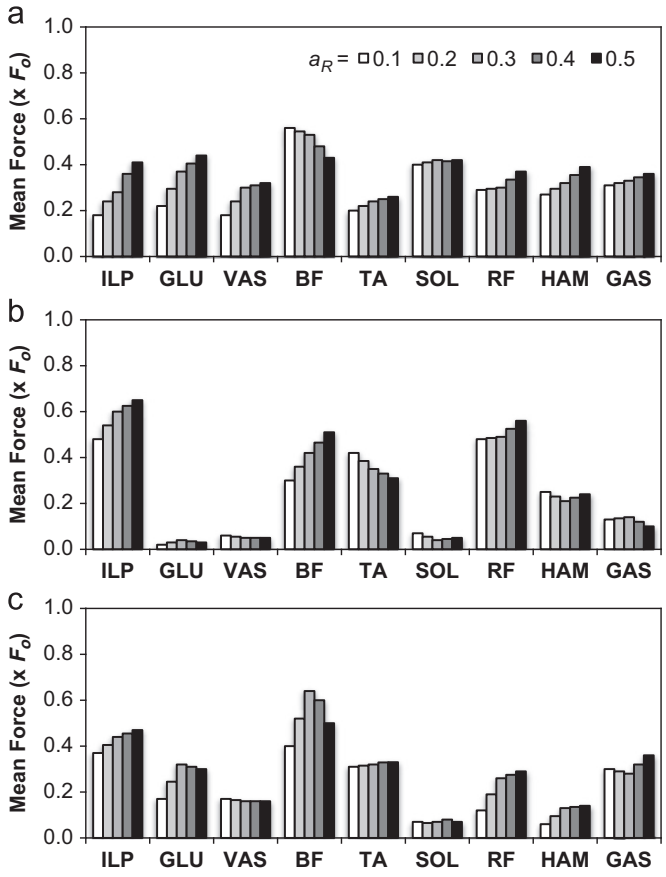

Fig. 7. Average (mean) muscle forces during (a) stance, (b) the first 50% of swing, and (c) the last 50% of swing as A_R was increased incrementally from 0.1 to 0.5. Darker shaded bars indicate greater A_R values. Force are scaled by F_o. Muscle abbreviations are as in Fig. 4.

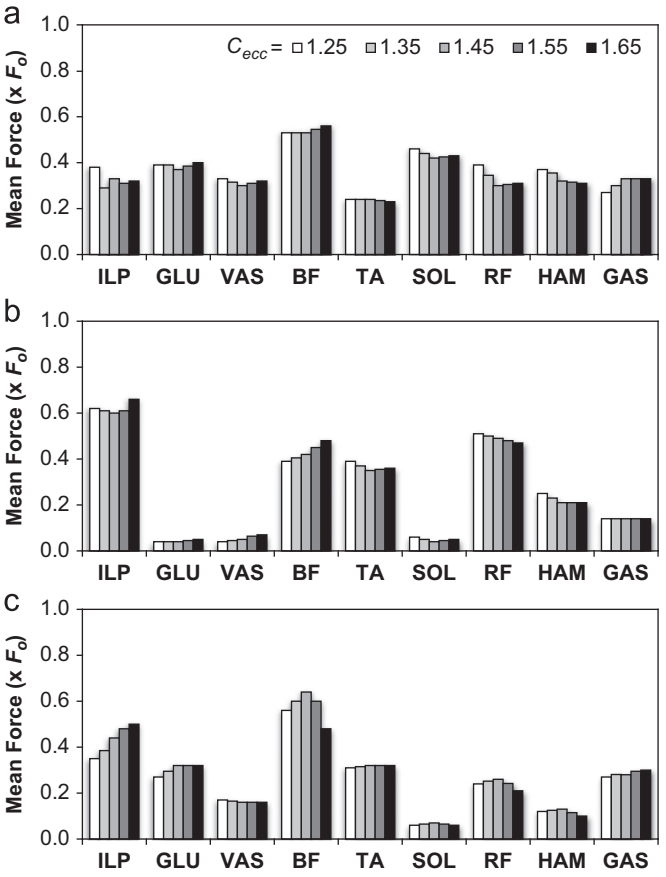

Fig. 8. Average (mean) muscle forces during (a) stance, (b) the first 50% of swing, and (c) the last 50% of swing as C_{ecc} was increased incrementally from 1.25 to 1.65. Darker shaded bars indicate greater C_{ecc} values. Force are scaled by F_o. Muscle abbreviations are as in Fig. 4.

affect concentric force production, they have their greatest effects at moderate and fast shortening velocities, respectively (Fig. 1). Because the muscle CCs tended to operate over a moderate range of shortening velocities (Figs. S1-S3), A_R should have the greatest potential for increasing sprinting speed. A greater range of speeds (5.22 to 6.91 m s^{-1}) was observed when V_{max} was manipulated compared to A_R (5.60 to 7.17 m s^{-1}), but this was due to the slow speeds that resulted when V_{max} was very low (e.g. 5.22 m s^{-1} when V_{max}=4 L_o s^{-1}), well below the range of V_{max} values typically used in forward dynamics simulations (10–12 L_o s^{-1}). Compared to A_R and V_{max}, the effect of C_{ecc} on sprinting speed was muted, suggesting a less important role in limiting maximum speed. Indeed, as sprinting speed increased, most muscle force increases occurred during concentric CC conditions.

By what mechanism does the force–velocity relationship limit sprinting speed? Weyand et al. (2000, 2010) suggested that sprinting speed is limited by the diminishing ability to support body weight due to decreased stance time as running speed increases. The finding that simulated speed increases were due primarily to increased stride length rather than stride frequency (i.e. the legs are not simply cycled more rapidly), along with the progressive increase in stance phase forces seen in some muscles, support this "time to generate force" theory. The stance phase forces of glutei and vasti, which contribute to body weight support in running (Hamner et al., 2010), tended to increase monotonically with sprinting speed. However, greater forces were also seen in the swing phase of the simulations. While Weyand et al. (2000, 2010) proposed that speed is limited centrally by stance phase dynamics, they noted that these dynamics also affect the time and muscular effort required in the subsequent swing phase.

The swing phase requires lower limb backward motion to be arrested and reversed after push-off, and the foot then re-positioned in preparation for the next stance phase. Chapman and Caldwell (1983) detailed the generation of lower limb kinetic energy in early swing to quickly propel the limb forward, followed by energy removal in late swing to arrest forward motion and accurately position the foot. The authors suggested that the hip flexors (iliopsoas, rectus femoris) were important for the early swing energy generation, with the knee flexors (including hamstrings) responsible for later energy dissipation. They proposed that this "energy management" task limits sprinting speed due to insufficient time for its completion as stride frequency increases and swing time decreases. However, in our simulations the duration of swing did not vary with speed (p=0.49, R^2=0.14), consistent with Weyand et al. (2000), who found that faster sprinters did not have shorter swing times.

In contrast, analysis of muscle forces supported Chapman and Caldwell's (1983) energy management theory. Increased speed was usually accompanied by increases in iliopsoas and biceps femoris forces in early swing, and by increases in knee flexor forces in late swing (Figs. 7 and 8). Biceps femoris activity in early swing tends to flex the knee and decrease lower limb moment of inertia, helping the hip flexors generate kinetic energy. Late swing knee flexor forces help to arrest this motion in preparation for foot contact. However, since the knee flexors are typically

lengthening in late swing, the lack of a strong relationship between C_{ecc} and sprinting speed suggests that the ability to dissipate kinetic energy in late swing plays at most a secondary role in limiting sprinting speed.

It should be noted that neither theory claims one phase (stance or swing) exclusively limits speed, nor does either preclude speed-limiting interactions between stance and swing. Our simulation results partially support both, and suggest a unified theory in which sprinting speed is limited by muscular ability to generate sufficient vertical impulse to support the body in stance and thus produce enough stride time to generate and dissipate the kinetic energy required for swing, similar to the argument briefly discussed by Weyand et al. (2000). Both tasks implicate the force–velocity relationship by requiring muscles to quickly generate large forces while they are shortening or lengthening rapidly. Based on our simulation results and the finding that muscle contractile components tended to shorten at moderate velocities regardless of the sprinting speed reached, we suggest that the shape parameter A_R plays an important role in modulating the ability of muscles to contribute to these tasks.

The speeds reached by the model ($\sim$7 m s^{-1}), with its parameters drawn from non-elite sprinters, were less than the speeds of elite human sprinters ($\sim$10–12 m s^{-1}). Simulations not shown here indicated that doubling the maximum isometric muscle forces permitted the model to reach elite speeds. While we would not expect qualitatively different results if the model's muscle strength was increased, caution should be exercised in extrapolating the present results to sprinters of different ability levels or using them to explain why elite sprint athletes are much faster than the rest of the population.

Our subjects likely ran below their absolute maximum speeds due to the relative short runway, although the experimental braking and propelling GRF impulses indicated nearly steady speeds for the measured step. However, the subject data were used only to define a starting point for the model's initial kinematic state, and this state was optimized along with the muscle excitations to maximize speed. Thus the lack of data from the subject's true maximum speeds is not a major limitation.

In summary, manipulation of the dynamic constant A_R resulted in the fastest maximum speed in forward dynamics simulations of human sprinting. Sprinting speed was also highly sensitive to the maximum shortening velocity V_{max}, while changes in the eccentric plateau C_{ecc} had a smaller effect. Most increases in the model's speed were due to longer stride lengths rather than greater stride frequencies. These results were due to the muscle CC velocities experienced during sprinting, which were moderate rather than high. Support was found at the individual muscle level for both the "time to generate force" (Weyand et al., 2000) and the "energy management" (Chapman & Caldwell, 1983) theories on how the force–velocity relationship limits maximum speed. However, the ability of the knee flexors to remove kinetic energy from the lower limb in late swing did not appear to be a critically limiting factor. The results suggest that sprinting speed may be optimally increased by focusing on increasing the stride length and the amount of muscle force that can be generated at moderate shortening velocities. It remains to be seen how these findings could be implemented in sprint training and conditioning programs.

Conflict of interest

The authors affirm that we have no personal or financial conflicts of interest related to the publication of this work.

Appendix A. Supplementary material

Supplementary data associated with this article can be found in the online version at doi:10.1016/j.jbiomech.2012.02.024.

References

Alexander, R.M., 2002. Tendon elasticity and muscle function. Comparative Biochemistry and Physiology A: Molecular and Integrative Physiology 133, 1001–1011.

Andersen, L.L., Andersen, J.L., Magnusson, S.P., Suetta, C., Madsen, J.L., Christensen, L.R., Aagaard, P., 2005. Changes in the human muscle force–velocity relationship in response to resistance training and subsequent detraining. Journal of Applied Physiology 99, 87–94.

Anderson, F.C., Pandy, M.G., 2001. Dynamic optimization of human walking. ASME Journal of Biomechanical Engineering 123, 381–390.

Chapman, A.E., Caldwell, G.E., 1983. Kinetic limitations to maximum sprinting speed. Journal of Biomechanics 16, 79–83.

Domire, Z.J., Challis, J.H., 2010. A critical examination of the maximum shortening velocity used in simulation models of human movement. Computer Methods in Biomechanics and Biomedical Engineering 13, 693–699.

Fenn, W.O., 1930a. Frictional and kinetic factors in the work of sprint running. American Journal of Physiology 92, 583–611.

Fenn, W.O., 1930b. Work against gravity and work due to velocity changes in running. American Journal of Physiology 93, 433–462.

Furusawa, K., Hill, A.V., Parkinson, J.L., 1927. The dynamics of sprint running. Proceedings of the Royal Society of London B 102, 29–42.

Hamner, S.R., Seth, A., Delp, S.L., 2010. Muscle contributions to propulsion and support during running. Journal of Biomechanics 43, 2709–2716.

Higginson, J.S., Neptune, R.R., Anderson, F.C., 2005. Simulated parallel annealing within a neighborhood for optimization of biomechanical systems. Journal of Biomechanics 38, 1938–1942.

Hill, A.V., 1938. The heat of shortening and the dynamic constants of muscle. Proceedings of the Royal Society of London B 126, 136–195.

Hof, A.L., 2003. Muscle mechanics and neuromuscular control. Journal of Biomechanics 36, 1031–1038.

Katz, B., 1939. The relation between force and speed in muscular contraction. Journal of Physiology 96, 45–64.

Lee, S.S., Piazza, S.J., 2009. Built for speed: musculoskeletal structure and sprinting ability. Journal of Experimental Biology 212, 3700–3707.

Mann, R.A., Hagy, J., 1980. Biomechanics of walking, running, and sprinting. American Journal of Sports Medicine 8, 345–350.

Miller, R.H., Caldwell, G.E., Van Emmerik, R.E.A., Umberger, B.R., Hamill, J., 2009. Ground reaction forces and lower extremity kinematics when running with suppressed arm swing. Journal of Biomechanical Engineering 131, 124502.

Miller, R.H., Umberger, B.R., Caldwell, G.E., 2011a. Limitations to maximum sprinting speed imposed by muscle mechanical properties. Journal of Biomechanics. doi:10.1016/j.jbiomech.2011.04.040.

Miller, R.H., Umberger, B.R., Hamill, J., Caldwell, G.E., 2011b. Evaluation of the minimum energy hypothesis and other potential optimality criteria for human running. Proceedings of the Royal Society B: Biological Sciences. doi:10.1098/rspb.2011.2015.

Neptune, R.R., Kautz, S.A., Zajac, F.E., 2001. Contributions of the individual ankle plantar flexors to support, forward progression and swing initiation during walking. Journal of Biomechanics 34, 1387–1398.

Riener, R., Edrich, T., 1999. Identification of passive elastic joint moments in the lower extremities. Journal of Biomechanics 32, 539–544.

Robertson, D.G.E., Caldwell, G.E., Hamill, J., Kamen, G., Whittlesey, S.N., 2004. Research Methods in Biomechanics. Human Kinetics, Champaign.

Thelen, D.G., Chumanov, E.S., Best, T.M., Swanson, S.C., Heiderscheit, B.C., 2005. Simulation of biceps femoris musculotendon mechanics during the swing phase of sprinting. Medicine and Science in Sports and Exercise 37, 1931–1938.

Thorstensson, A., Larsson, L., Tesch, P., Karlsson, J., 1977. Muscle strength and fiber composition in athletes and sedentary men. Medicine and Science in Sports 9, 26–30.

Umberger, B.R., 2010. Stance and swing phase costs in human walking. Journal of the Royal Society Interface 7, 1329–1340.

Umberger, B.R., Gerritsen, K.G.M., Martin, P.E., 2003. A model of human muscle energy expenditure. Computer Methods in Biomechanics and Biomedical Engineering 6, 99–111.

Van Ingen Schenau, G.J., de Koning, J.J., de Groot, G., 1994. Optimisation of sprinting performance in running, cycling and speed skating. Sports Medicine 17, 259–275.

Van Soest, A.J., Bobbert, M.F., 1993. The contributions of muscle properties in the control of explosive movements. Biological Cybernetics 69, 195–204.

Weyand, P.G., Bundle, M.W., 2005. Energetics of high-speed running: integrating classical theory with contemporary observations. American Journal of Physiology—RICP 288, R956–R965.

Weyand, P.G., Sandell, R.F., Prime, D.N., Bundle, M.W., 2010. The biological limits to running speed are imposed from the ground up. Journal of Applied Physiology 108, 950–961.

Weyand, P.G., Sternlight, D.B., Bellizzi, M.J., Wright, S., 2000. Faster top running speeds are achieved with greater ground forces not more rapid leg movements. Journal of Applied Physiology 89, 1991–1999.

Winters, J.M., Stark, L., 1985. Analysis of fundamental human movement patterns through the use of in-depth antagonistic muscle models. IEEE Transactions on Biomedical Engineering 52, 826–839.

Winters, J.M., Stark, L., 1988. Estimated mechanical properties of synergistic muscles involved in movements of a variety of human joints. Journal of Biomechanics 21, 1027–1041.

Zajac, F.E., 1989. Muscle and tendon: properties, models, scaling, and application to biomechanics and motor control. Critical Reviews in Biomedical Engineering 17, 359–411.